LDPC Coded OFDM System Design and Performance Verification on a Realistic Underwater Acoustic Channel Model

Hyeong-Won Jeon, Su-Je Lee, and Heung-No Lee*
School of Information and Communications, GIST,
Oryong-dong, Buk-gu, Gwangju 500-712, Republic of Korea
{hyeongwon, sujerago, heungno*}@gist.ac.kr

Abstract— **The underwater acoustic channel (UAC) is highly frequency selective; the degree of selectiveness depends on a detailed geometry of the channel. Further, the response changes over time as conditions affecting the response (such as water temperature, sea surface wind, salinity, etc.) are time-varying. A system design to deal with the frequency and time selective channel in UAC, therefore, becomes very challenging. We consider low density parity check (LDPC) coded orthogonal frequency division multiplexing (OFDM) system to deal with deep sub-band fading problems. In this paper, we aim to, first, provide a detailed realistic UAC model as we have noted that most LDPC coded OFDM systems have not been tested under realistic channels; second, to design a robust LDPC coded OFDM system; and third to test the proposed system under a variety of conditions using the channel model. We show robustness of the proposed system in simulation under a number of realistic channel conditions.**

I. INTRODUCTION

As interest increases in marine resources and environment, underwater communication is obtaining popularity for a variety of applications (ocean surveyor, data acquisition, marine pollution monitoring, disaster prevention, navigation, etc.); expanding this research area beyond just the previous military surveillance [1].

UAC is complex and has difficulty maintaining robustness as the channel conditions affecting the response (e.g., water temperature, sea surface wind and salinity) are time-varying. In particular, the multipath delay spread that comes from the reflection causes inter-symbol interference (ISI) and frequency selective fading, consequently leading to system performance falloff. Furthermore, the time selective fading and the Doppler spread caused by time-varying sea surface wind and moving fluids instigate system performance degradation [2][3].

In the special case that time variation of the channel is sufficiently slower than the symbol rate, the frequency selective fading is surmountable via OFDM system [4]. For OFDM systems, it is known that deep fading at certain specific sub-carriers is detrimental to system performance. To mitigate this negative effect, error correction codes such as convolutional codes, Reed-Solomon codes, turbo codes, and LDPC codes are usually used [4][5].

Under OFDM systems operating over UAC, the Doppler spread comes from the drift of the underwater node and surface buoy can easily destroy orthogonality. Moreover, a long guard period is needed, since the relatively slow propagation speed causes a large maximum delay spread. There have been approaches to solve this orthogonality destruction problem caused by the frequency offset. The authors in [6] suggested using the orthogonal matching pursuit (OMP) algorithm based on the channel estimation. Other approaches include adaptive phase synchronization on the time domain [7] and adaptive OFDM signal detection algorithm [8]. The application of such system designs that depend on synchronization and frequency offset equalization is limited because of its high complexity. In this paper we circumvent this problem by selecting the OFDM system parameters carefully (see Section III).

There have been papers using the binary LDPC codes [9] and non-binary LDPC codes [5] in OFDM systems over UAC. However, in these previous works, there were many cases using channel models that were overly simplified to test the system performance, e.g., (*i*) employing too little multipath components; (*ii*) overlooking the channel variation according to the positional change in the configuration of the node and buoy.

In this paper, we aim to (*i*) model a realistic simulation channel against which a proposed system can be verified; (*ii*) design an LDPC coded OFDM system that works well under a realistic channel. This system design can overcome the frequency selective fading, as well as time selective fading problems at the same time (within a 15 m/s maximum sea surface wind speed); and (*iii*) show the robust performance of our designed system under realistic channel settings.

This paper is organized as follows. We describe a realistic simulation channel model in section II. We present the system parameter settings and the simulation results in section III. Finally, our conclusions are contained in section IV.

II. CHANNEL ANALYSIS AND MODELING

A. Doppler Spread

The surface scattering of UAC depends on the sea surface condition. Under an ideally flat surface condition, incident waves are almost perfectly reflected with π phase shifting.

However, under practical conditions, swells lead to movement of the reflection point and create energy dispersion. The Doppler spread with a carrier frequency f kHz [10] is represented as follows.

$$f_D = (0.0175/c) f \cdot w^{3/2} \cdot \cos\theta\,, \tag{1}$$

where c, w and θ are sound speed, sea surface wind speed and grazing angle, respectively. Sound speed is affected by salinity, water temperature, pressure, etc., but it is 1500 m/s under normal conditions.

Fig. 1 is the Doppler spread against the carrier frequency and sea surface wind speed when we assume $\cos\theta = 1$ in (1). This figure denotes a geometric Doppler spread increase using a higher carrier frequency. Although using a higher carrier frequency has an advantage (i.e., increase of available transmission bandwidth), it also has a disadvantage (i.e., geometric increase of the Doppler spread). Thus, this trade-off relationship should be considered on the communication system design over UAC.

B. *Multipath*

Acoustic waves in UAC are reflected on the sea surface and ocean bottom, as well as forming multipath, as shown Fig. 2. The transfer function of the reflection path with distance l_p, where $p = 0, 1, 2, \cdots$ [11] is

$$\overline{H}_p(f) = \frac{\Gamma_p}{\sqrt{A(l_p, f)}}\,, \tag{2}$$

where $A(l_p, f)$ is the single path attenuation with distance l_p m and carrier frequency f Hz. In addition, Γ_p is the reflection coefficient determined by the number of reflections on the sea surface n_{sp} and bottom n_{bp} [11].

In (2), the single path loss $A(l_p, f)$ is

$$A(l, f) = A_0 \cdot l^k \cdot a(f)^l\,, \tag{3}$$

where A_0 is a constant scaling factor and k is a spreading factor between 1 and 2, according to the type of spreading. In this paper, we set A_0 as 1 and k as 2 with consideration of the spherical spreading. $a(f)$ is an absorption coefficient expressed as follows.

$$a(f) = 10^{\alpha(f/1000)/10000} \tag{4}$$

In (4), $\alpha(f)$ is defined by Thorp's empirical formula [12].

$$\alpha(f) = 0.11\frac{f^2}{1+f^2} + 44\frac{f^2}{4100+f^2} + 2.75\cdot 10^{-4}\cdot f^2 + 0.003 \tag{5}$$

In (2), the reflection coefficient Γ_p is

$$\Gamma_p = \gamma_s^{\,n_{sp}} \gamma_b^{\,n_{bp}}(\theta_p)\,, \tag{6}$$

where γ_s and γ_b are the reflection coefficients at the sea surface and bottom, respectively. Under an ideally flat surface condition, γ_s is approximated as -1 and γ_b is calculated as follows.

$$\gamma_b(\theta) = \begin{cases} \dfrac{\rho_b \sin\theta - \rho\sqrt{(c/c_b)^2 - \cos^2\theta}}{\rho_b \sin\theta + \rho\sqrt{(c/c_b)^2 - \cos^2\theta}} & ,\cos\theta \le c/c_b \\ 1 & otherwise \end{cases}, \tag{7}$$

where ρ and c are the general water density and sound speed; and, ρ_b and c_b are the density and sound speed at the sea bottom. Normally, these are 1000 g/m^3, 1500 m/s, 1800 g/m^3 and 1300 m/s, respectively.

The impulse response considering this reflection characteristic in UAC is

$$h(t) = \sum_p h_p(t - \tau_p)\,, \tag{8}$$

where h_p is an inverse Fourier Transform (IFT) result of each transfer function and $\tau_p = (l_p - l_0)/c$ is an arrival time gag between the direct path and each reflection path.

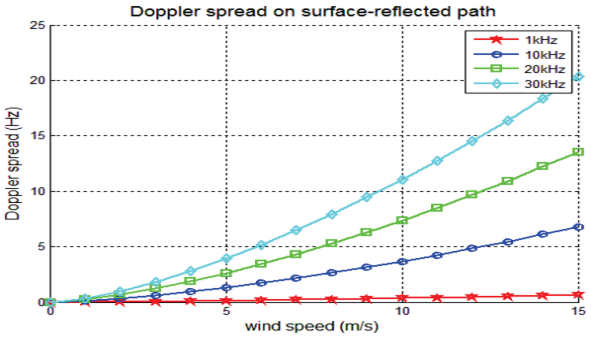

Figure 1. Doppler spread caused by reflection on the sea surface.

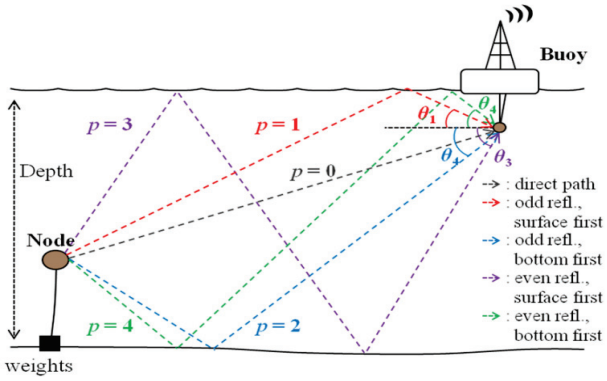

Figure 2. Multipath in UAC.

C. *Simulation channel modeling*

UAC modeling is extremely complex and difficult, since the conditions affecting the channel (such as geometry of the channel, wave height changed by sea surface wind, spatial position changed by sea current, etc.) need to be considered. Thus, there are many problems and difficulties in applying all conditions to channel modeling. In this paper, the simulation channel is modeled assuming ideally flat surface and bottom conditions, invariable positioning of the node and buoy and a maximum sea surface wind speed of 15 m/s.

Fig. 3 shows simulation channel models having a water depth of 50 m, with 1000 m separating the node and buoy. In Fig. 3 (a) the node and buoy are fixed at 7 m and 45 m from the bottom, respectively. Fig. 3 (b)-(d) are similar to Fig. 3 (a), except that each channel has depth changes to the node and buoy (i.e., in the case of Fig. 3 (b), the depth of the node is 0 m (meaning it is located on the ocean bottom); in Fig. 3 (c), the depth of buoy is 50 m (meaning it is located on the sea surface); In Fig. 3 (d), the depth of the node and buoy is changed to 0 m and 50 m, respectively.)

Fig. 4 (a) shows the multipath having an odd number of reflections. In detail, path ray (i) is a case where the first reflection occurred on the sea surface and path ray (ii) is a case where the first reflection occurred on the ocean bottom. Similarly, Fig. 4 (b) shows the multipath having an even number of reflections. In path ray (iii) and path ray (iv), the first reflection occurred on the sea surface and ocean bottom, respectively. There are infinitely many multipath that can came from reflection on the sea surface and bottom, but we only considered those paths within a 30 dB energy gap against the direct path.

Fig. 5 (a)-(d) are impulse responses of the simulation channels shown in Fig. 3. Via analysis of these results, the maximum delay spread and coherence bandwidth are guessable as about 25 ms and 40 Hz, respectively. In addition, Fig. 5 (b)-(d) shows the limited multipath creation according to the position of the node and buoy. In the impulse response of the Fig. 3 (b) channel, i.e., Fig. 5 (b), the multipath occurring with the first reflection on the ocean bottom (path ray (ii) and (iv) in Fig. 4) is limited since the node is located on the ocean bottom. Similarly, in the Fig. 3 (c) channel, i.e., Fig. 5 (c), the multipath having a last reflection on the sea surface (path ray (i) and (iv) in Fig. 4) cannot be created since the buoy is located on the sea surface. For the same reasons, looking at the channel in Fig. 3 (d), creation of multipath occurring with the first reflection on the ocean bottom and the last reflection on the sea surface is limited. Consequently, in special cases, such as when the node and buoy are located on the sea surface and/or ocean bottom, even though the change of the node and buoy depth is small, causes the wide performance variation.

III. CODED OFDM SYSTEM DESIGN

A. *OFDM system parameter design*

In OFDM systems, adjusting transmission bandwidth, and the symbol duration, is needed so that orthogonality among sub-carriers is maintained since such a system is very sensitive for inter-channel interference (ICI) caused by frequency offset.

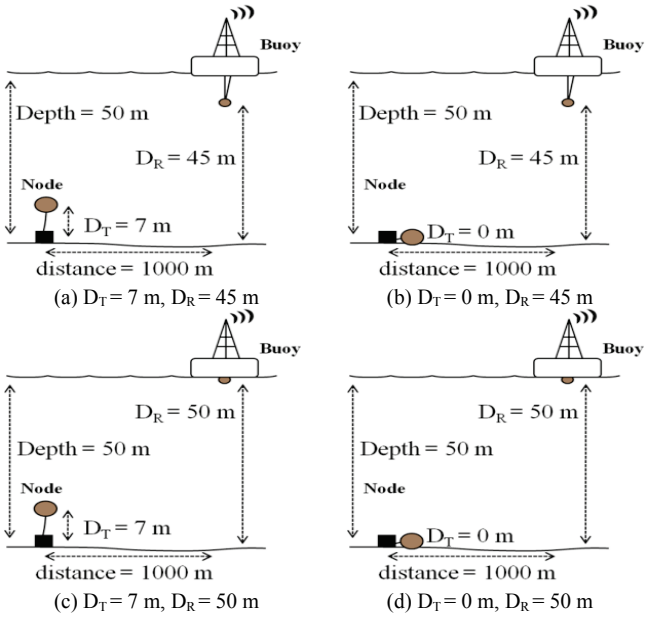

(a) D_T = 7 m, D_R = 45 m (b) D_T = 0 m, D_R = 45 m

(c) D_T = 7 m, D_R = 50 m (d) D_T = 0 m, D_R = 50 m

Figure 3. Simulation UAC model concept.

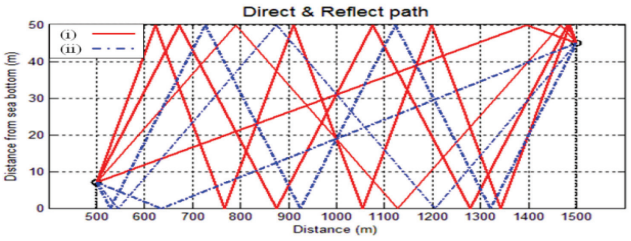

(a) Multipath having odd number reflection

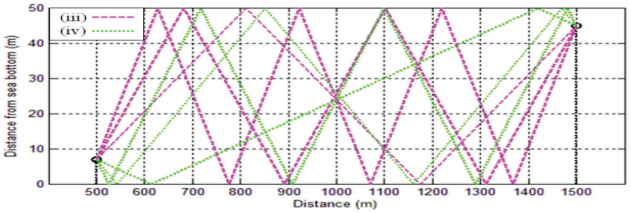

(b) Multipath having even number reflection

Figure 4. The multipath of the simulation UAC model.

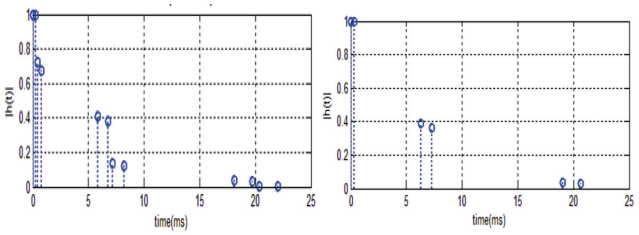

(a) D_T = 7 m, D_R = 45 m (b) D_T = 0 m, D_R = 45 m

(c) D_T = 7 m, D_R = 50 m (d) D_T = 0 m, D_R = 50 m

Figure 5. The impulse response of the simulation UAC model.

In addition, the insertion of the guard period that is longer than or equal to the maximum delay spread is needed between connected symbols to solve the ISI. The back part of a valid symbol is copied and inserted as the cyclic prefix (CP) [13].

Table 1 represents the system parameters considering discussed so far. As we mentioned above in section II, since Doppler spread increases geometrically, as the carrier frequency increases, to overcome time selective fading, we should select a carrier frequency that is as low as possible. However, the use of a carrier frequency that is too low causes a decline of the available bandwidth. In this paper, we chose a 7 kHz carrier frequency assuming the use of 10 kHz bandwidth. To overcome the ISI problem, we set the CP period as 25 ms based on the simulation results of the modeled channels. Under such a setting, the maximum delay spread and coherent time of the channel are about 4.744 Hz and 210 ms, respectively. It is essential to choose a number of sub-carriers that satisfy conditions to overcome the frequency selective fading ($\Delta f < B_C$) and time selective fading ($T_S \ll T_C$) [14] at the same time. In this paper, we chose 256 sub-carriers to satisfy these conditions.

The suggested OFDM is able to overcome not only frequency selective fading, since the sub-carrier bandwidth (39.0625 Hz) is smaller than coherent bandwidth of channel (40 Hz); but also ISI, since CP period (25 ms) is larger than maximum delay spread; as well as time selective fading, since the OFDM symbol duration (50.6 ms) is sufficiently smaller than the coherent time of channel (210 ms).

Fig. 6 shows the bit error rate (BER) of the simulation results in UAC. It also shows the system performance improvement via the OFDM system but there is about 8 dB SNR variation, according to channels, at the 10^{-3} BER point.

B. *Coded OFDM system*

The LDPC codes used in this paper were suggested by R. G. Gallager in 1962 and known as one of the most advanced error correction codes. The parity check matrix H of the LDPC codes consists of numerous zeroes and only a few ones in a kind of sparse matrix. Commonly, regular LDPC codes are represented as (n, j, k) where n is block length and j and k are the number of ones on each row and column of the parity check matrix, respectively [15]. As the j and k parameters increase, the minimum distance of the codes increase, but we cannot guarantee the work of the iterative decoder, because the parity check matrix is too dense. Thus, in this paper, we consider this trade-off relationship and set the parameters of j and k to 4 and 8, respectively. Further, we set block size n to 256. These are the same as the number of sub-carriers to combine with the previously designed OFDM system.

Fig. 7 is a block diagram of the suggested coded OFDM system using the regular LDPC code. The input data sequence m is multiplied with generator matrix G_{sys}, and then constructs c_t. After BPSK modulation, c_t is assigned to each sub-carrier.

$$c_t = mG_{sys}\ ,\ t = 1, 2, \cdots, n \tag{12}$$

$$d_t = 2c_t - 1 \tag{13}$$

TABLE I. THE OFDM SYSTEM PARAMETERS

Parameter	Value
Carrier frequency	7 kHz
Transmission bandwidth : BW	10 kHz
Maximum Doppler Spread : $B\tau_{max}$	4.744 Hz
Coherent Time : $T_C = 1/B\tau_{max}$	210 ms
Maximum Delay Spread : τ_{max}	25 ms
Coherent Bandwidth : $B_C = 1/\tau_{max}$	40 Hz
Number of sub-carriers : N_{FFT}	256
Sub-carrier bandwidth : $\Delta f = BW/N_{FFT}$	39.0625Hz
Valid symbol duration : $T_D = 1/\Delta f$	25.6 ms
CP period : $T_{CP} \geq \tau_{max}$	25 ms
OFDM symbol duration : $T_S = T_D + T_{CP}$	50.6 ms

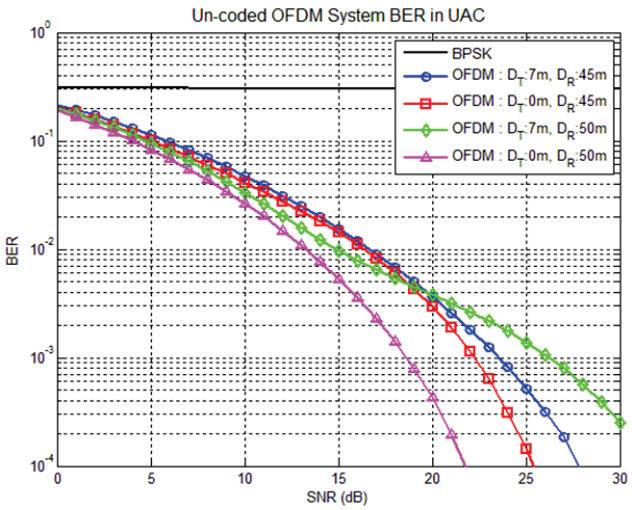

Figure 6. The BER of the simulation channels.

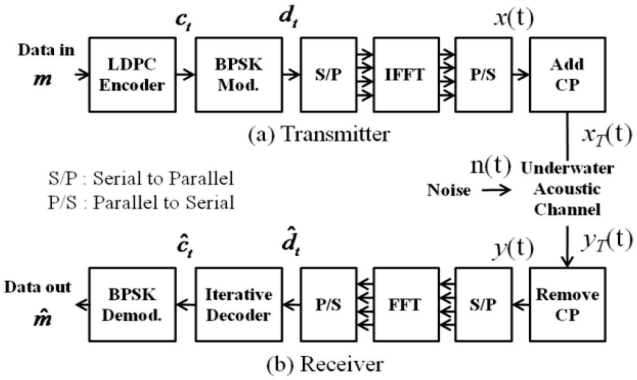

Figure 7. System block diagram.

The received digital signal on frequency domain is

$$Y[k] = H[k]d_t + N[k]\ , \tag{14}$$

where $H[k]$ and $N[k]$ are Fourier transform results of the impulse response and sampled noise, respectively.

The equalized signal $\hat{d}_t$ is

$$\hat{d}_t = \Re eal\left\{\frac{Y[k]}{\hat{H}[k]}\right\}, \quad (15)$$

where $Y[k]$ and $\hat{H}[k]$ are the received signal and estimated channel transfer function, respectively. In this paper, we assume perfect channel estimation, i.e., $\hat{H}[k] = H[k]$. Such $\hat{d}_t$ is used to set the initial log likelihood ratio (LLR) values at the iterative decoder. The iterative decoder gradually renews LLR values via message passing [16] and decided as zero or one.

C. System Performance Verification

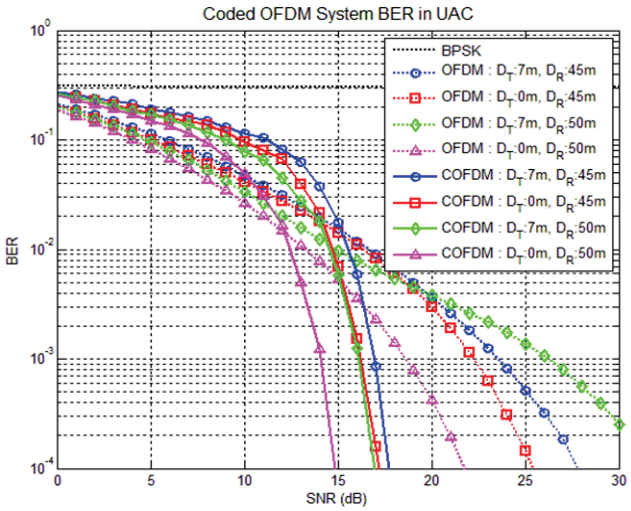

Figure 8. The BER of the simulation channels (with 10 iterations).

Fig. 8 shows the BER performance of the suggested system. These results show the overcoming of the performance falloff via the LDPC coded OFDM system. In detail, over a certain threshold of received SNR, this system is able to solve the performance falloff problem. To be specific, this system not only achieved a 7 dB SNR benefit, but also reduced the SNR variation, according to channels, from 8 dB to 3 dB at the 10^{-3} BER point versus the un-coded OFDM system.

IV. CONCLUSION

In this paper, we provided a realistic UAC model for simulation and designed an LDPC coded OFDM system that works well under the realistic channel. We selected the system parameters, as shown in the Table.1, to overcome the frequency selective fading and time selective fading at the same time, up to a sea surface wind speed of less than 15 m/s. As stated above section II, the small positional change of the node and buoy is able to lead to the wide performance variation. We showed the proposed system reduced such performance variation by using the LDPC code. The proposed system not only achieved a 7 dB SNR benefit compared to the un-coded OFDM system but also reduced the SNR variation from 8 dB to 3 dB at the 10^{-3} BER point.

ACKNOWLEDGMENT

This research was supported by Leading Foreign Research Institute Recruitment Program through the National Research Foundation of Korea (NRF) funded by the Ministry of Education, Science and Technology (MEST) (K20902001632-10E0100-06010). This research was supported by the National Research Foundation of Korea (NRF) grant funded by the Korea government (MEST) (N0. 2011-0016496)

REFERENCES

[1] I. F. Akyildiz, D. Pompili, and T. Melodia, "Underwater acoustic sensor networks: research challenges," *Ad Hoc Networks Journal*, Elsevier, vol. 3, Issue 3, pp. 257-279, Mar. 2005.

[2] I. F. Akyildiz, D. Pompili, and T. Melodia, "Challenges for efficient communication in underwater acoustic sensor networks," *ACM SIGBED* Rev., vol. 1, no. 2, pp. 3-8, Jul. 2004.

[3] M. Stojanovic and J. Preisig, "Underwater acoustic communication channels: Propagation models and statistical characterization," *IEEE Communications Magazine*, vol. 47, no. 1, pp. 84-89, Jan. 2009.

[4] L. Litwin and M. Pugel, "The Principles of OFDM," *RF Signal Processing*, pp. 30-48, Jan. 2001.

[5] J. Huang, S. Zhou, and P. Willett, "Nonbinary LDPC coding for multicarrier underwater acoustic communication," *IEEE JSAC Special Issue on Underwater Wireless Communications and Networks*, vol. 26, no. 9, pp. 1684–1696, Dec. 2008.

[6] S. Mason, C. Berger, S. Zhou, K. Ball, L. Freitag, and P. Willett, "An OFDM design for underwater acoustic channels with Doppler spread," in *Proc. of the 13th DSP Workshop*, Marco Island, FL, Jan. 2009.

[7] M. Stojanovic, "OFDM for underwater acoustic communications: Adaptive synchronization and sparse channel estimation," in Proc. of International Conference on Acoustics, Speech and Signal Proc., Las Vegas, NV, Apr. 2008.

[8] M. Stojanovic, "Low complexity OFDM detector for underwater channels," in *Proc. of MTS/IEEE OCEANS conference*, Boston, MA, Sep. 2006.

[9] Li-yang Bai, Fang Xu, Ru Xu, Shao-yu Zheng, "LDPC Application Based on CI/OFDM Underwater Acoustic Communication System," *icise*, pp.2641-2644, 2009 First International Conference on Information Science and Engineering, 2009.

[10] M. Stojanovic, "Underwater Acoustic Communication," entry in *Encyclopedia of Electrical and Electronics Engineering*, John G. Webster, Ed., John Wiley & Sons, 1999, vol. 22, pp. 688-698.

[11] P. Qarabaqi and M. Stojanovic, "Statistical modeling of a Shallow Water Acoustic Communication Channel," in *Proc. Underwater Acoustic Measurements Conference*, Nafplion, Greece, Jun. 2009.

[12] L. Berkhovskikh and Y. Lysanov, *Fundamentals of Ocean Acoustics*, Springer, 1982..

[13] O. Edfors, M. Sandell, J. van de Beek, D. Landstrom, and F. Sjoberg, *An introduction to orthogonal frequency-division multiplexing*, Technical report, Lulea University of Technology, Sep. 1996.

[14] B. Sklar, Digital Communications: *Fundamentals and Applications*, 2nd Ed., Prentice Hall, 2001.

[15] R. G. Gallager, "Low density parity check codes," *IRE Trans. Inform. Theory*, vol. IT-8, pp. 21-28, Jan. 1962.

[16] H. N. Lee, *Wireless Communications Class lecture notes*, Spring Semester, GIST, 2010.